Theor Chem Acc (2011) 128:497–503
DOI 10.1007/s00214-010-0852-1

REGULAR ARTICLE

A density functional theory study of the manganese-phthalocyanine

Daniele Stradi · Cristina Díaz · Fernando Martín · Manuel Alcamí

Received: 30 July 2010 / Accepted: 31 October 2010 / Published online: 16 December 2010

Abstract We present a systematic density functional theory (DFT) study of the isolated manganese-phthalocyanine, MnPc, by using both localized gaussian-type orbital (GTO) and plane-wave (PW) basis sets and the following exchange-correlation functionals: B3LYP, PBE, PBE0, HSE, and HSE06. We find a very good agreement between GTO and PW results, which is a necessary condition in order to extend the present methodology to MnPc molecules deposited on metal surfaces. We conclude that the HSE06 functional is the most suitable one for the study of MnPc/inorganic interfaces with a basis of plane waves. We compare our calculated electron energy spectra with two available experiments [Kraus et al. in Chem Phys Lett 469:121, 2009; Grobosch et al. in Organics Electron 11:1483, 2010; Papageorgiou et al. in Prog Surf Sci 77:139, 2004] in which the ultraviolet photoemission spectra (UPS) have been measured. Our results suggest that spectra obtained from MnPc molecules in the gas phase are closer to those obtained from thin films of MnPc deposited on inert surfaces than to those obtained from thick films. Finally, we report optical absorption spectra by using a time-dependent DFT approach. Our results are again compatible with measurements performed on thin MnPc films.

Published as part of the special issue celebrating theoretical and computational chemistry in Spain.

D. Stradi (✉) · F. Martín
Instituto Madrileño de Estudios Avanzados en Nanociencias (IMDEA-Nanociencia), Cantoblanco, Madrid 2849, Spain
e-mail: daniele.stradi@uam.es

D. Stradi · C. Díaz · F. Martín · M. Alcamí
Departamento de Química, Universidad Autónoma de Madrid, Módulo 13, Madrid 28049, Spain

Keywords Mn-phthalocyanine · DFT · Hybrid and non-hybrid functionals

1 Introduction

Phthalocyanines (Pc's) are a prototypical class of organic porphyrin derivatives, which can combine with almost any metal in the periodic table forming highly (thermically and chemically) stable complexes, widely used, for example, as pigments, dyes or photoelectronic devices [4, 5]. These complexes have a planar structure where the central metal atom is constrained by the π-conjugated macrocyclic ligand, and the interaction between the central metal ion and the organic macrocycle determines the spin configuration of the complex.

Metal-phthalocyanines (MPc's) were already studied in the 60's and the 70's (see, for instance, [6–10]). During the last decade, they have been object of a renewed interest due to their potential use in nanoscale technologies, such as field-effect transistors, light-emitting diodes, photovoltaic and solar cells, or gas sensors [11, 12]. Furthermore, MPc's deposited on metal substrates are considered prototypical models of semiconductor/metal interfaces for molecular electronic applications such as organic electronic devices [13, 14]. As prototypical single-molecule magnets, MPc's also have a wide applicability in molecular spintronics [15–17].

The interest aroused by the MPc's in the last few years is unquestionable, as evidenced by the significant number of both experimental and theoretical studies present in the literature. From an experimental point of view, the first studies of MPc's adsorbed on surfaces using scanning tunneling microscopy (STM) go back to the 80's [18], but it is nowadays that these kind of studies, as well as those performed using scanning tunneling spectroscopy (STS),

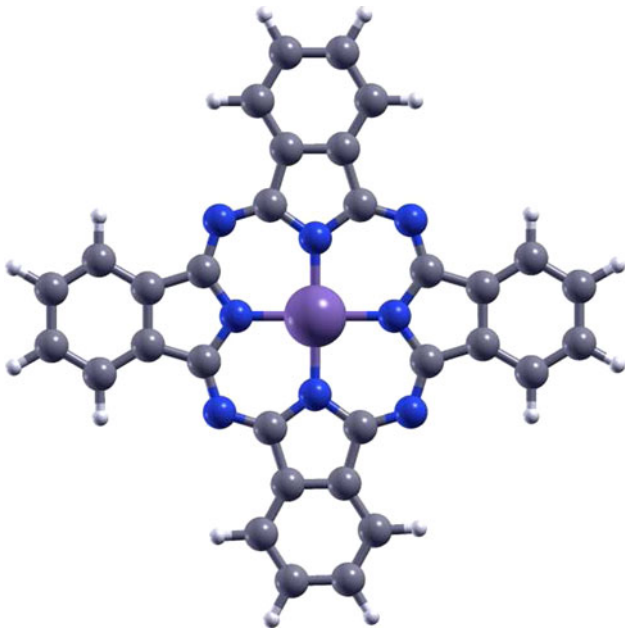

Fig. 1 Schematics of the geometry of MnPc. Mn, N, C and H atoms are represented in *violet*, *blue*, *gray* and *white*, respectively

are experiencing a real boom [13, 19–32]. For example, STM and STS measurements on Kondo effect, resonance and temperature [22, 24, 28] have revealed a meaningful number of magnetic properties of MPc's adsorbed on metal substrates. Between these magnetic MPc's, MnPc, which is the object of the present study, is considered the prototype molecular magnet [33] (see Fig. 1).

This large amount of experimental studies on MPc/surface systems requires a parallel development of theoretical methods allowing an appropriate analysis of the experimental observations, as well as a further understanding of the physical phenomena behind them. The major challenge for the theoretical methods in this field is to describe the properties of these molecules when deposited on metallic surfaces. This implies to get simultaneously an accurate description of both the organic molecule and the metal surface. The use of DFT (density functional theory) [34] in this context is unavoidable due to the dimensions of the systems involved. Within DFT, different formalisms can be adopted to describe the electronic exchange-correlation (XC) and the performance of a functional greatly depends on the characteristics of the molecules. For instance, the semiempirical hybrid functional B3LYP (Becke 3-parameter Lee-Yang-Parr) [35, 36], which has almost become a standard when dealing with organic molecules, is not suitable to describe metals as discussed in detail by Paier et al. [37]. In the case of MPc, Marom et al. [38–40] have performed an extensive theoretical study focused on the performance of a number of XC functionals. Among the standard GGA functionals tested, the PBE (Perdew-Burke-Hernerzhof) [41], which is the most commonly used in describing organic-metal systems [24, 42–44], has been shown to yield very good optimized geometries for MPc's, but a remarkably altered orbital ordering [38], as well as underbound localized orbitals, due to self-interaction errors [45]. Such problems are alleviated by its parameter-free hybrid variant, PBEh [46–48]. Marom et al. [38] have proposed the HSE (Heyd-Scuseria-Ernzernhof) screened hybrid functional [49] as the best choice to study CuPc/metal surfaces, because of the reasonable description of the electronic structure on both sides of the CuPc/inorganic interface. A simpler though less accurate solution has been proposed from an extension of the local density approximation (LDA) [50].

For gas phase isolated NiPc and CoPc molecules [39], the molecular geometry has been found to be well described by the PBE functional, but reasonable electronic structures are only obtained by employing hybrid functionals (B3LYP, PBEh and M06 [51]). On the other hand, electronic structure studies of isolated MnPc and FePc in gas phase [40] have not driven, hitherto, to any conclusive result. In particular, for the isolated MnPc molecule considered in this work, results in the literature are contradictory: a very recent theoretical study [17] suggests, in disagreement with previous results mentioned above [38, 42], that the PBE functional is the appropriate choice. To complicate the situation, comparison with experimental results is rather indirect, since no data for gas phase MnPc are available. Calculated electronic spectra are usually compared with Ultraviolet Photoemission Spectra (UPS) obtained from films of MnPc deposited on "inert" inorganic surfaces, although it should be noticed that photoemission data do not represent the electronic density of states (DOS), but the DOS multiplied by a cross-section, which has a particular photon energy dependence that is different for states of different atoms. Very recent spectra obtained from thin MnPc films [1, 2] exhibit a dominant peak at $\sim$7 eV and a much smaller peak at $\sim$4 eV, while the opposite has been found from thick MnPc films [3]. Kraus et al. [1] and Grobosch et al. [2] have also measured optical absorption spectra and electron energy-loss spectra (EELS) from thin MnPc films and have found that they are very similar. The results in Ref. [2] also show the fundamental role played by the central metal ion in the electronic structure of MnPc: by a combined spectrocopic investigation using energy-loss spectroscopy and photoemission spectroscopy over a whole set of MPc, it is evidenced how the subtle interaction between the metal and the ligand results in profound differences between their electronic structure, making every single MPc a case study on the theoretical point of view. However, so far no theoretical attempt has been reported to compare with these measurements.

In this work, we try to shed more light on the MnPc problem by considering the following aspects. Firstly, we

will revisit the problem of the appropriate choice of the XC functional by considering a few more functionals than in [38] and by comparing results obtained from localized (Gaussian-Type Orbitals, GTO) and plane-wave (PW) basis sets. The latter comparison is a basic step in order to extend the present methodology to MnPc molecules deposited on metal surfaces. Secondly, we will compare our calculated electron spectra with two existing UPS experiments [1–3] and thus analyze their appropriateness to extract information that is also meaningful for MnPC in the gas phase. Finally, we will also evaluate optical absorption spectra in order to compare with the available experimental data. To achieve these goals, we have carried out systematic DFT calculations for isolated MnPC by using both GTO and PW basis and the following XC functionals: B3LYP [35], PBE [41], PBE0 [46], HSE [49], and HSE06 [52], to describe the electronic structure of the MnPc.

The paper is organized as follows. In the next section, we present the computational methods used in this work. We present and discuss the results in Sect. 3 Finally, we end with some conclusions in Sect. 4.

2 Computational details

We have compared DFT calculations performed within both GTO and PW formalisms. The former is the method of choice to study isolated molecular species, whereas the latter allows one to study periodic systems with considerable band dispersion, such as metallic surfaces.

Unrestricted-DFT (UDFT) GTO calculations were performed, for the gas phase isolated MnPc molecule, using Gaussian 09 [53]. It must be pointed out that in addition to the above mentioned problems, related to the correct choice of the exchange-correlation functional, it has been also shown that the overall electronic structure of MnPc exhibits a high dependence on the quality of the basis set employed [39]. Thus, all UDFT calculations were performed using a high quality correlation-consistent cc-pVTZ basis on Mn. This basis set includes 4d2f1g shells on Mn. The rest of the atoms were treated with two different basis sets: a double-zeta (6–31G(d,p)) or a triple-zeta (cc-pVTZ). The use of these two basis sets has allowed us to test the influence of the ligand basis set on the electronic structure.

Spin-Polarized PW calculations were performed by means of the VASP code [54]. In this case, the molecule was placed parallel to the xy-plane, with the Mn atom at the center of the plane. A supercell of $24 \times 24 \times 10$ Å^3 was used in order to minimize the interaction between molecules lying in neighboring cells. The ionic cores were described by the Projector Augmented Wave (PAW) method [55], and the kinetic energy cutoff for the plane waves expansion was set to 415 eV. For a sufficiently large energy cutoff, PW basis sets are effectively complete. However, when PAW potentials are employed, substantially larger values of the energy cutoff must be used to properly generate the PAW projectors. Since the supercell is very large, it was enough to sample the Brillouin zone at the Γ-point. A gaussian smearing of $\sigma = 0.05$ eV was applied.

The MnPc geometry was optimized at the PBE level of theory for the GTO and the PW basis sets; the subsequent comparison between results obtained with different functionals was conducted on these structures. This approach is supported by previous calculations in closely related systems, showing that the difference between optimized geometries with hybrid and non-hybrid functionals is almost negligible [38, 56]. Although a few functionals may predict slightly distorted geometries showing non-physical symmetry breaking, the influence of this problem in the simulated UPS spectra is also negligible [40].

Vertical excitation energies and oscillator strengths that are necessary to obtain the optical absorption spectrum were evaluated within the time-dependent DFT (TDDFT) formalism [57, 58] by using Gaussian 09 [53].

3 Results and discussion

Figure 2 shows the calculated eigenvalue spectra obtained using UDFT/GTO, for different functionals and basis sets, together with the UPS data for MnPc thin films [1, 2] and for thick MnPc films [3]. The spectra on thin and thick films differ in the relative intensity of the bands. Previous theoretical calculations [40] have only compared with thick film results [3], which were the only ones available in those days. In order to simulate the experimental resolution, the theoretical spectra have been convoluted with gaussian functions. It should be noticed that the comparison between Khon-Sham eigenvalues and UPS data is rather reasonable because Kohn-Sham eigenvalues are good approximations to electron removal energies, as it has been already proved for similar cases involving metal-Phthalocyanines and related carbon-based molecules [38, 39, 45, 59]. From Fig. 2, it can be seen that PBE (Fig. 2b) is not a suitable exchange-correlation functional, since it fails, even qualitatively, in describing the main features of either UPS spectrum, e.g., the position of the peaks located around $E - E_{\mathrm{HOMO}} = -2.5$ eV and $E - E_{\mathrm{HOMO}} = -5.5$ eV. In particular, the PBE calculated spectrum is clearly compressed by about 20% with respect to the experiment, as already noticed by Marom et al. [39]. Switching to the PBE0 functional, while maintaining the same basis set (6–31G(d,p) on the ligand), results in an overall stretching of the eigenvalue spectrum and improves the agreement with the experimental results. When the quality of the basis set is improved by using for the ligand the same basis set as for the metal (cc-pVTZ), the agreement

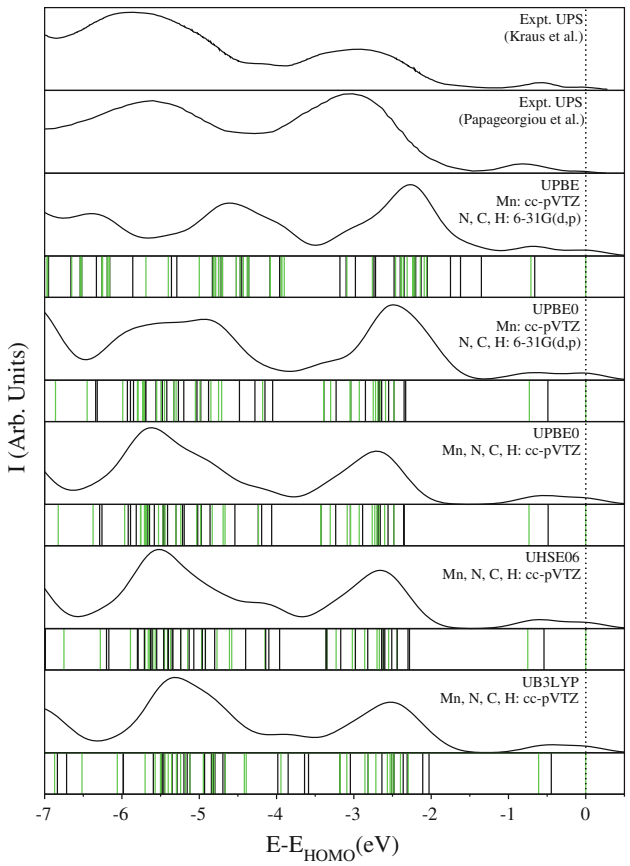

Fig. 2 MnPc eigenvalue spectra (*black*: spin α, *green*: spin β), calculated with UDFT/GTO using different exchange-correlation functionals and basis sets, and convoluted results with a gaussian function of width 0.25 eV to be compared with the UPS data of Refs. [1–3], which are also shown in the figure

with experiment also improves, especially with the UPS spectrum reported for thin films [1, 2]. In this case, the two main features of the experimental UPS spectrum are correctly reproduced, both their position and relative intensity. Screening the exact exchange by using the HSE functional results in an even better agreement with the experimental results of [1, 2], since minor characteristics of the spectrum, such as the shoulder appearing at around $E - E_{\mathrm{HOMO}} = -4\,\mathrm{eV}$, and the small difference between the peaks at about $E - E_{\mathrm{HOMO}} = -0.5\,\mathrm{eV}$ and about $E - E_{\mathrm{HOMO}} = 0.0\,\mathrm{eV}$ are better reproduced than in the spectrum obtained with standard PBE0. These results suggest that thin films of MnPc preserve most of the features observed in the UPS spectrum of gas phase MnPc.

The B3LYP-based calculated spectrum is also in very good agreement with the experimental spectra of [1, 2]. For this latter functional, results not shown here reveal that the influence of a lower quality basis set for the ligand on the electronic structure of MnPc is much less pronounced than for the other functionals, but, as already stressed, the poor performance of B3LYP for metals should prevent one to use it to study MnPc/metal surface systems. These results point out the subtle interplay between different factors that can influence the electronic structure of MnPc, and likely of other metal-phthalocyanines. The HOMO-LUMO gaps calculated with the different exchange-correlation functionals are, respectively, 0.21 eV (PBE), 1.48 eV (PBE0), 1.33 eV (B3LYP), and 0.82 eV (HSE). These calculated gap energies follow nicely the trend in HOMO-LUMO gap energy obtained by Marom et al. for CuPc [38].

We now turn our attention to the analysis of the spectra obtained with PW basis sets. The comparison PW and GTO calculations must be done with some caution, since, apart from the obvious differences in the basis characteristics, PW calculations require some additional approximations. Paier et al. [60] have observed that, with PBE and PBE0 functionals, PAW-PW and GTO calculations yield similar results only when a large aug-cc-pVQZ basis set is used for the latter. More important is the fact that PAW-PW calculations rely on the frozen-core approximation (the ionic cores are described by using the PAW method), contrary to the all-electrons GTO-type calculations. We have tested the ability of PAW-PW calculations to reproduce GTO results by performing a systematic analysis similar to that already discussed for the GTO calculations. The results of this analysis are shown in Fig. 3.

Figure 3 shows that, as for GTO basis sets, PW results obtained with the PBE functional disagree with the experimental data. We observe that the entire eigenvalue spectrum is shifted to higher energies with respect to the experiments, pointing out the clear deficiency of the standard semilocal functionals such as PBE in the description of the electronic structure of MnPc, irrespectively of the basis set employed. In Fig. 3, we also show an explicit comparison between the results obtained with GTO and PW basis sets by using the same PBE0 functional. Although small differences can be observed all along the electronic spectrum, the convoluted spectrum calculated at the PAW-PW-PBE0 level is also in good agreement with the experiment of Kraus et al. [1] and Grobosch et al. [2] (although the relative intensity of the dominant peaks seems to be better reproduced by the GTO-PBE0 calculations). The calculated HOMO-LUMO gap energies, for PAW-PW calculations, are 0.19 eV (PBE) and 1.49 eV (PBE0), in agreement with the GTO calculations. In view of the effective completeness of the cc-pVTZ and PW basis sets, the origin of these small differences are likely due to the use of the PAW method to describe the ionic cores in the PW calculations.

In Fig. 3, we can also see the comparison between the occupied eigenvalue spectra obtained with the PBE0 and HSE functionals. Two spectra computed with HSE are shown: one obtained with standard HSE-06 and the other one obtained by using a slightly increased screening

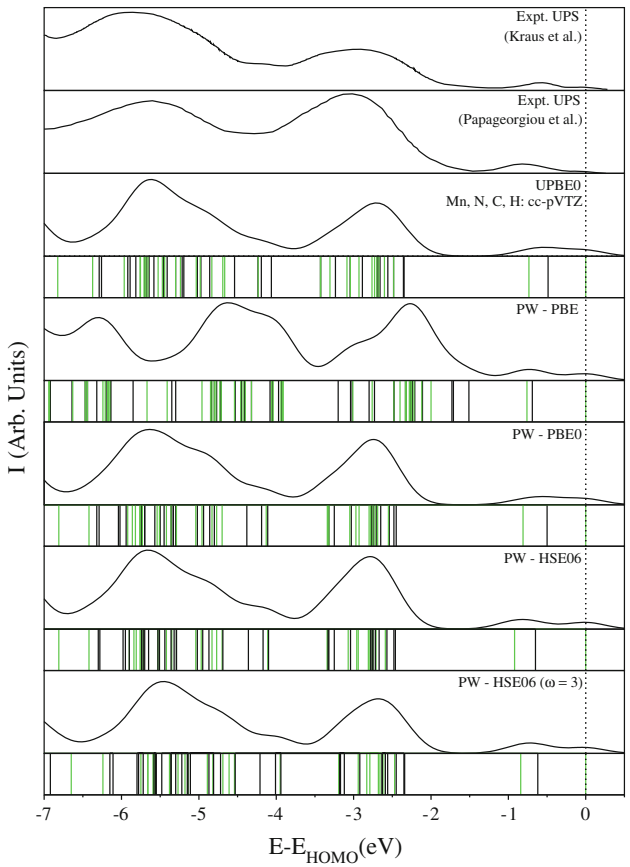

Fig. 3 Calculated eigenvalues spectra (*black*: spin α; *green*: spin β) for GTO-PBE0 (Mn, N, C, H: cc-TVZ), PAW-PW-PBE, PAW-PW-PBE0, and PAW-PW-HSE06, and convoluted results with a gaussian function of width 0.25 eV to be compared with the UPS data of Refs. [1–3], which are also shown in the figure

parameter $\omega = 0.3\,\text{Å}^{-1}$. In general, similarly to that observed in the case of GTO calculations, screening the exact exchange does not introduces significant changes in the occupied eigenvalue spectrum calculated with PBE0. The agreement with experiment is slightly improved, although the comparison is still slightly worse than for GTO-HSE calculations (see Fig. 2). As for PBE0, the PAW-PW-HSE06 calculations make a slightly poorer job than GTO-HSE-06 calculations in reproducing the relative intensity of the two low-lying peaks. However, this can be improved by increasing the value of the screening parameter: as Fig. 3 shows the relative intensity of the two major peaks around $E - E_{\text{HOMO}} = -2.75\,\text{eV}$ and $E - E_{\text{HOMO}} = -5.5\,\text{eV}$, as well as that of the HOMO peak and the small peak around $E - E_{\text{HOMO}} = 0.75\,\text{eV}$, appear to be reproduced satisfactorily. Consistently with the GTO results, screening non-local exchange reduces significantly the HOMO-LUMO gap, which is calculated to be 0.77 and 0.7 eV for HSE06 and HSE06 ($\omega = 3\,\text{Å}^{-1}$) functional, respectively.

The DOS obtained with the different functionals in the PW calculations (see Fig. 4) exhibits features similar to

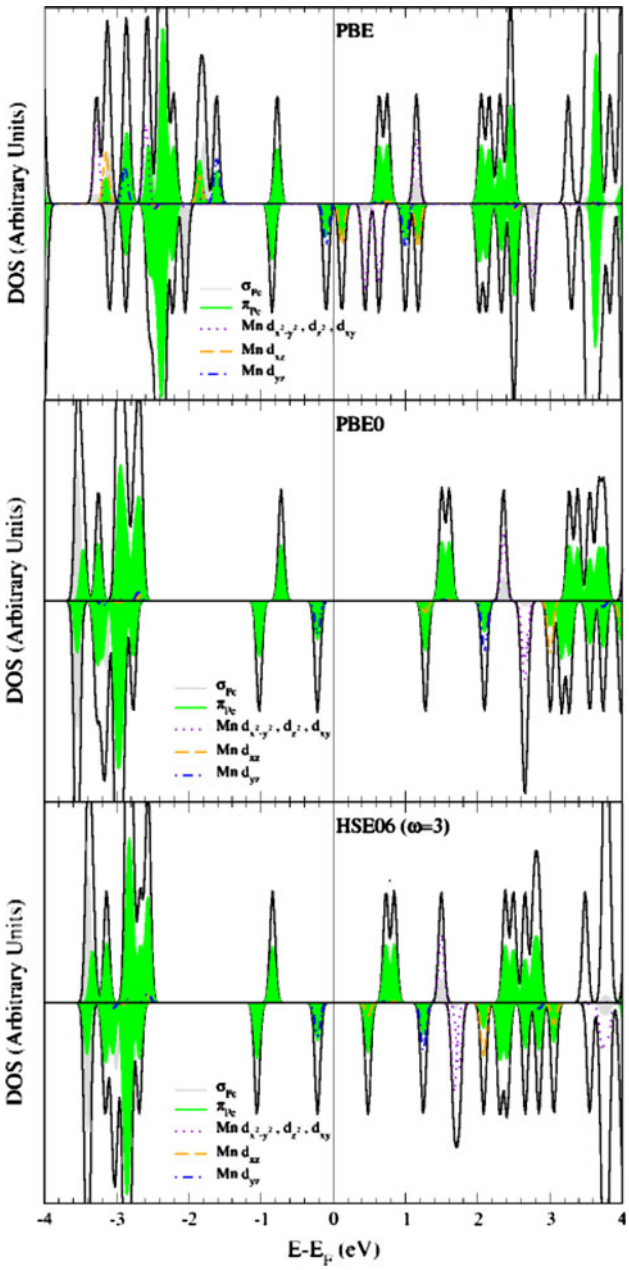

Fig. 4 Projected Density Of States of MnPC, for PBE, PBE0, and HSE06 ($\omega = 3\ \text{Å}^{-1}$) functionals. Energy is scaled with respect to the Fermi level E_F. Upper part of the figures corresponds to beta spins, lower part to alpha spins

those of the simulated UPS spectra. Consistently with the eigenvalues spectra and the HOMO-LUMO gap values discussed above, the DOS evaluated at the PBE level of theory appears to be compressed in a smaller energy window compared to the DOS calculated employing hybrid functionals. On the other hand, the DOS calculated with PBE0 and HSE are very similar, the only appreciable difference between them being the HOMO-LUMO energy gap width. Substantial differences are observed between the DOS evaluated with PBE and with hybrid functionals. In fact, the

only electronic levels that seem to be reproduced consistently by both approaches are the HOMO and the a_1u orbitals localized at $E - E_{HOMO} = -1$ eV. The LUMO has also the same character in all cases, but the relative contribution of the d_{xz} orbital of the central manganese atom to this orbital is much lower in the PBE case than in the hybrid cases. Interestingly, qualitative differences can be observed in the unoccupied DOS between the hybrid and non-hybrid cases. In particular, for PBE0-DOS, the first group of unoccupied orbitals splits in two distinct subgroups, one located roughly 2.2 eV above the Fermi level, which can be identified with levels showing significant contribution from the π-directed orbitals of the organic ligand and the Mn d_{xz} and d_{yz} orbitals. And the other one located in the energy range [2.2–2.8 eV] above the Fermi level, which is formed by electronic levels having significant contribution from the σ-directed orbitals of the organic ligand and the Mn $d_{x^2-y^2}$, d_{z^2} and d_{xy} orbitals. This order is completely lost in the case of PBE calculations. The same differences are also observed between the unoccupied eigenvalue spectra of non-hybrid PBE/cc-pTVZ and hybrid PBE0/cc-pVTZ and HSE06/cc-pVTZ calculations.

In order to confirm the accuracy of the electronic structure obtained with hybrid PBE0 and HSE06 functionals, we have computed the vertical excitation energies and oscillator strengths by using TDDFT [57, 58] with a cc-pVTZ basis set starting from the converged PBE0/cc-pVTZ and HSE06/cc-pVTZ structures. In Fig. 5, we compare the results with the experimental spectra measured by Kraus et al. in Ref. [1]. From this figure, it can be seen that the excitation energies relative to the adsorption peaks located around 1.75 and 2.15 eV and the shoulder located around 1.45 eV, are well reproduced, albeit with a small tendency to overestimate them. At energies below 1 eV, the agreement is less satisfactory since the transitions within the [0.5–1.0 eV] energy range appear to be forbidden, contrary to experiment where small peaks associated with intramolecular excitations are observed. This discrepancy with the experiment can be attributed either to the molecule's interaction in the solid films, either to the shortcomings of the TDDFT method, which is known to generally underestimate the oscillator strengths, or both.

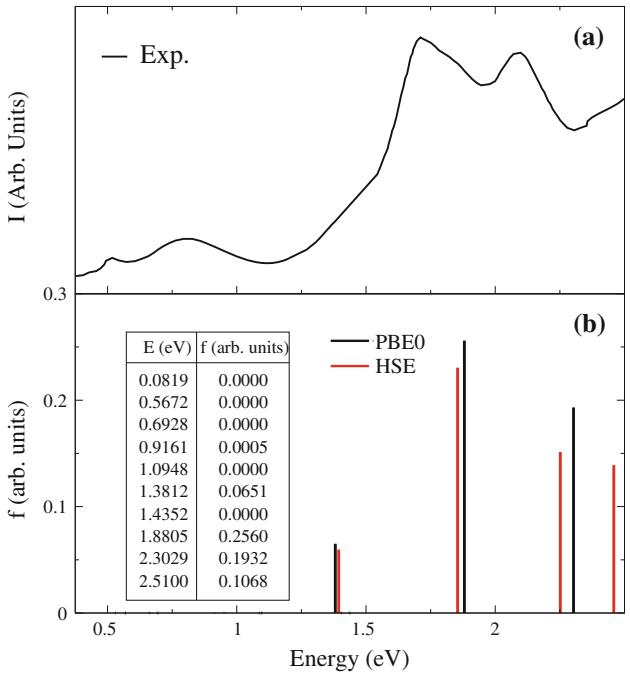

E (eV)	f (arb. units)
0.0819	0.0000
0.5672	0.0000
0.6928	0.0000
0.9161	0.0005
1.0948	0.0000
1.3812	0.0651
1.4352	0.0000
1.8805	0.2560
2.3029	0.1932
2.5100	0.1068

Fig. 5 Excitation energies and relative oscillator strengths obtained from PBE0/cc-pVTZ and HSE06/cc-pVTZ calculations, compared with optical absorption spectra of Ref. [1]. The *inset* shows the PBE0 numerical data for the oscillator strengths

4 Conclusions

We have performed a systematic study on the electronic structure of MnPc, benchmarking our results against recent experimental UPS data available in literature [1–3]. Since the ultimate goal is to describe the molecule adsorbed on a metallic surface, we have compared the performance of Gaussian-Type Orbitals (GTO) calculations, the *standard* method when dealing with isolated gas phase species, and Plane Waves (PW), which are commonly used for metal surfaces. Since the main difficulty is to achieve an accurate description of both sides of the organic/metal interface, we have checked the performance, on the electronic structure of MnPc, of exchange-correlation functionals which are known to perform well for metals. In particular, we have compared the results obtained with the non-hybrid GGA (generalized gradient approximation) PBE functional and the hybrid functionals PBE0 and HSE06. Generally speaking, PW calculations agree reasonably well with GTO calculations. In agreement with results obtained previously for similar phthalocyanines using the same functionals [38, 56], we have found that the screened hybrid HSE06 functional gives the overall best results. Reasonably good results are also obtained in the case of the hybrid PBE0. On the other hand, the standard GGA-PBE functional, which was suggested as the more suitable exchange-correlation functional [17] to deal with MnPc's, fails in describing the electronic structure, giving a general upshift toward higher energies of the overall electronic spectrum. The comparison with available UPS measurements [1–3] suggests that spectra obtained from MnPc molecules in the gas phase are closer to those obtained from thin films of MnPc molecules deposited on inert surfaces than to those obtained from thick films.

In order to further confirm the validity of the results obtained for the occupied part of the electronic spectrum of the molecule, we have also performed TDDFT (time-dependent

density functional theory) calculations at the PBE0/cc-pVTZ and HSE06/cc-pVTZ levels. The computed excitation energies and oscillator strengths agree reasonably well with the experimental ones obtained from thin MnPc films, despite the fact that the low-lying weak transitions observed in the experiment are theoretically predicted as forbidden, probably due to shortcomings of the TDDFT method. Finally, based on our calculations, we point to the HSE06 functional as the most appropriate one to study MnPc's/inorganic interfaces with a basis of plane waves.

Acknowledgments We thank Mare Nostrum BSC and CCC-UAM for allocation of computer time. Work partially supported by the European COST Action CM0702, the Ministerio de Ciencia e Innovación through the DGI projects Nos. FIS2007-60064 and CSD 2007-00010 and the DGCI project No. ACI2008-0777, and the Comunidad Autónoma de Madrid through the DGI project S2009/MAT1726.

References

1. Kraus R, Grobosch M, Knupfer M (2009) Chem Phys Lett 469:121
2. Grobosch M, Schmidt C, Kraus R, Knupfer M (2010) Organics Electron 11:1483
3. Papageorgiou N, Salomon E, Angot T, Layet J, Giovanelli L, Lay GL (2004) Prog Surf Sci 77:139
4. Orti E, Bredas JL (1992) J Am Chem Soc 114:8669
5. Yamashita A, Hayashi T (1996) Adv Mater 8:791
6. Hudson A, Whitfield HJ (1967) Inorg Chem 6:1120
7. Moss TH, Robinson AB (1968) Inorg Chem 7:1692
8. Dale BW, Williams RJP, Edwards PR, Johnson CE (1968) J Chem Phys 49:3445
9. Barraclough CG, Martin RL, Mitra S, Sherwood RC (1970) J Chem Phys 53:1643
10. Kirner JF, Dong W, Scheidt WR (1976) Inorg Chem 15:1685
11. Kadish KM, Smith KM, Guilard R (2003) Applications of Phthalocyanines. The prophyrin handbook, vol 19. Academic Press, San Diego
12. Crone B, Dodabalapur A, Lin YY, Filas RW, Bao Z, LaDuca A, Sarperhkar R, Katz HE, Li W (2000) Nature 403:521
13. Nazin GV, Qui XH, Ho W (2003) Science 307:77
14. Witte G, Wöll C (2004) J Mater Res 19:1889
15. Wende H, Bernien M, Luo J, Sorg C, Ponpandiard N, Kurde J, Miguel J, Piantek M, Xu X, Eckhold P, Kuch W, Baberschke K, Panchmatia PM, Sanyal B, Oppeneer PM, Eriksson O (2007) Nat Mater 6:516
16. Bogani L, Wernsdorfer W (2008) Nat Mater 7:179
17. Shen X, Sun L, Benassi E, Shen Z, Zhao X, Sanvito S, Hou S (2010) J Chem Phys 132:054703
18. Lippel PH, Wilson RJ, Miller MD, Wöll C, Chiang S (1989) Phys Rev Lett 62:171
19. Tu XW, Mikaekian GR, Ho W (2008) Phys Rev Lett 100:126807
20. Nazin GV, Wu SW, Ho W (2005) Proc Natl Acad Sci 102:8832
21. Jiang P, Ma X, Ning Y, Song C, Chen X, Jia JF, Xue QK (2008) J Am Chem Soc 130:7790
22. Zhao A, Li Q, Chen L, Xiang H, Pan S, Wang B, Xiao X, Yang J, Hou JG, Zhu Q (2005) Science 309:1542
23. Iacovita C, Rastei MV, Heinrich BW, Brummen T, Kortus J, Limot L, Bucher JP (2008) Phys Rev Lett 101:116602
24. Gao L, Ji W, Hu YB, Cheng ZH, Deng ZT, Liu Q, Jiang N, Lin X, Guo W, Du SX, Ans WAH, Xie XC, Gao HJ (2007) Phys Rev Lett 99:106402
25. Cheng ZH, Gao L, Deng ZT, Jiang N, Lin X, He XB, Du SX, Gao HJ (2007) J Phys Chem C 111:9240
26. Copakumar TG, Lackinger M, Hackert M, Müller F, Hietschold M (2004) J Phys Chem B 108:7839
27. Koudia M, Abel M, Maurel C, Bliek A, Catalin C, Mossoyan M, Mossoyan JC, Porte L (2006) J Phys Chem B 110:10058
28. Fu YS, Ji SH, Chem C, Ma XC, Wu R, Wang CC, Duan WH, Qiu XH, Sun B, Zhang P, Jia JF, Xue QK (2007) Phys Rev Lett 99:2566601
29. Wu SW, Nazin GV, Chem X, Qui XH, Ho W (2004) Phys Rev Lett 93:236802
30. Vitali L, Fabris S, Conte AM, Brink S, Ruben M, Baroni S, Kern K (2008) Nano Lett 8:3364
31. Chang S, Kuck S, Brede J, Lichtenstein L, Hoffmann G, Wiesendanger R (2008) Phys Rev B 78:233409
32. Tsukahara N, Noto KI, Ohara M, Shiroki S, Takagi N (2009) Phys Rev Lett 102:167203
33. Mitra S, Gregson A, Hatfield W, Weller R (1983) Inorg Chem 22:1729
34. Kohn W, Sham LJ (1965) Phys Rev 140:A1133
35. Becke AD (1993) J Chem Phys 98:5648
36. Stephens PJ, Devlin FJ, Chabalowski CP, Frisch MJ (1994) J Phys Chem 98:11623
37. Paier J, Marsman M, Kresse G (2007) J Chem Phys 127:024103
38. Marom N, Hod O, Scuseria GE, Kronik L (2008) J Chem Phys 128:164107
39. Marom N, Kronik L (2009) Appl Phys A 95:159
40. Marom N, Kronik L (2009) Appl Phys A 95:165
41. Perdew JP, Burke K, Ernzerhof M (1996) Phys Rev Lett 77:3865
42. Calzolari A, Ferretti A, Nardelli MB (2007) Nanotechnologies 18:424013
43. Calzolari A, Jim W, Reutt-Robey JE, Nardelli MB (2007) Nanotechnologies 18:424013
44. Wang J, Shi Y, Cao J, Wu R (2009) Appl Phys Lett 94:122502
45. Dori N, Menon M et al (2006) Phys Rev B 73:195208
46. Adamo C, Barone V (1999) Chem Phys Lett 314:1999
47. Adamo C, Barone V (1999) J Chem Phys 110:6158
48. Perdew JP, Ernzerhof M, Burke K (1996) J Chem Phys 105:9982
49. Heyd J, Scuseria GE, Ernzerhof M (2003) J Chem Phys 118:8207
50. Vázquez H, Jelinek P, Brandbyge M, Jauho A, Flores F (2009) Appl Phys A 95:257
51. Zhao Y, Truhlar DG (2008) Acc Chem Res 41:157
52. Krukau AV, Vydrov OA, Izmaylov AF, Scuseria GE (2006) J Chem Phys 125:224106
53. Frisch MJ, Trucks GW et al (2009) Gaussian 09 Revision a.1. Gaussian Inc, Wallingford
54. Kresse G, Hafner J (1993) Phys Rev B 47:558
55. Blochl PE (1994) Phys Rev B 50:17953
56. Marom N, Tkatchenko A, Scheffler M, Kronik L (2010) J Chem Theory Comput 6:81
57. Casida ME, Jamorski C, Casida KC, Salahub DR (1998) J Chem Phys 108:4439
58. Onida G, Reining L, Rubio A (2002) Rev Mod Phys 74:601
59. Palummo M, Hogan C, Sottile F, Bagalá P, Rubio A (2009) J Chem Phys 131:084102
60. Paier J, Hirschl R, Marsman M, Kresse G (2005) J Chem Phys 122:234102